Menara Perkebunan 2024, 92(1), 70-81
p-ISSN: 0125-9318/ e-ISSN: 1858-3768
DOI: http://dx.doi.org/10.22302/iribb.jur.mp.v92il.561
Accreditation Number: 164/E/KPT/2021

In silico study: molecular docking of SARS-Cov-2 endoribonuclease on active compounds of *Gmelina arborea* Roxb. bark

Studi in silico*: penambatan molekuler protein endoribonuklease SARS-CoV-2 terhadap senyawa aktif kulit kayu* Gmelina arborea *Roxb.*

Shobiroh NUUR'ALIMAH, Agnia Nurul JANNATI, Laksmi AMBARSARI*) & Syamsul FALAH

Department of Biochemistry, Faculty of Mathematics and Natural Sciences, IPB University, Jl. Raya Dramaga, Bogor 16680, Indonesia

Received 8 Dec 2023 / Revised 4 Apr 2024 / Accepted 19 Apr 2024

Abstrak

*Infeksi oleh SARS-CoV-2 (*severe acute respiratory syndrome coronavirus *2) memicu penyakit COVID-19 pada saluran pernapasan serupa pneumonia. Virus ini mengkode empat protein struktural serta 16 protein non-struktural (nsp), salah satunya nsp15 atau endoribonuklease (NendoU). NendoU berperan penting dalam replikasi dan transkripsi virus serta mengurangi stimulasi terhadap respon sel imun. Senyawa aktif dalam kulit kayu* Gmelina arborea *Roxb. memiliki kandungan antioksidan yang dapat menghambat aktivitas NendoU SARS-CoV-2. Penelitian ini bertujuan menganalisis potensi senyawa dari kulit kayu* Gmelina arborea *Roxb. dalam menghambat NendoU SARS-CoV-2 secara* in silico *dengan aplikasi YASARA Structure. Balnophonin merupakan ligan uji terbaik berdasarkan nilai ΔG pengikatan, konstanta disosiasi (Kd), prediksi karakteristik fisikokimia, farmakokinetik, dan toksisitas. Oleh karena itu, balanonphonin dapat dikembangkan sebagai obat alternatif yang efektif dalam menghambat NendoU SARS CoV-2.*

[Kata kunci: antioksidan, COVID-19, in silico*, NendoU]*

Abstract

Infection by SARS-CoV-2 (severe acute respiratory syndrome coronavirus 2) triggers COVID-19 disease of the respiratory tract similar to pneumonia. The virus encodes four structural proteins and 16 non-structural proteins (nsp), one of which includes nsp15 or endoribonuclease (NendoU). NendoU plays an important role in viral replication and transcription and reduces the stimulation of immune cell responses. Active compounds in *Gmelina arborea* Roxb. bark have antioxidant properties that can inhibit the NendoU activity of SARS-CoV-2. This study aims to analyze the potential of compounds from *Gmelina arborea* Roxb. bark in inhibiting SARS-CoV-2 NendoU within in silico using the YASARA structure application. Balnophonin is the best test ligand based on binding ΔG value, dissociation constant (Kd), prediction of physicochemical characteristics, pharmacokinetics, and toxicity. Therefore, balanophonin can be developed as an effective alternative drug to inhibit SARS CoV-2 NendoU.

[Keywords: antioxidant, COVID-19, in silico, NendoU]

Introduction

SARS-CoV-2 (severe acute respiratory syndrome coronavirus 2) is a virus that causes respiratory infections similar to pneumonia, which is now called COVID-19 (coronavirus disease 2019). The disease was first identified in Wuhan, China, in December 2019 and spread rapidly throughout the world that in January 2020, the World Health Organization (WHO) declared COVID-19 as a public health emergency (Handayani et al., 2020; Aditia, 2021). SARS-CoV-2 is composed of four structural proteins, including spike protein (S), envelope (E), membrane (M), and nucleocapsid (N), as well as 16 non-structural proteins (nsp), one of which is nsp15 or endoribonuclease (NendoU) (Boophati et al., 2020).

Endoribonuclease (NendoU) is an essential protein and highly conserved in all coronaviruses (CoVs) and plays an important role in viral replication and transcription. The protein cleaves the

*) Korespondensi penulis: laksmi@apps.ipb.ac.id

Menara Perkebunan is DOAJ indexed Journal and accredited as Sinta 2 Journal (https://sinta.kemdikbud.go.id/journals/profile/3125)
How to Cite: Nuur'alimah, S., Jannati, A. N., Ambarsari, L., & Falah, S. (2024). In silico study: molecular docking of endoribonuclease SARS-Cov-2 on active compounds of *Gmelina arborea* Roxb. bark. *Menara Perkebunan*, *92*(1), 70-81.
http://dx.doi.org/10.22302/iribb.jur.mp.v92il.561

polyuridylate sequences in negative-sense viral RNA, limiting its length and abundance. This mechanism reduces stimulation of the interferon (IFN) immune cell response, thus blocking or inhibiting the activation of the MDA5 sensor in host cells (Mandilara et al., 2021). The docking of drug compounds on these proteins has the potential to inhibit the SARS-CoV-2 replication process in host cells, especially at the catalytic site (Khan et al., 2021). According to Deng et al. (2019), loss of NendoU function will result in a protective immune response. Therefore, inhibition of endoribonuclease makes it an effective therapeutic agent for COVID-19.

Several active compounds from natural materials were reported to be effective in inhibiting SARS-CoV and MERS-CoV. These compounds can be tested against SARS-CoV-2 which has genetic similarities with the two viruses (Septiana, 2020). One of the natural ingredients with various benefits is white teak (*Gmelina arborea* Roxb.). According to Falah et al. (2008), one part of white teak that is widely used for traditional medicine is its bark. Active compounds in white teak bark are known to have high antioxidant activities. According to Fedoreyev et al. (2018), antivirals and antioxidants have a close relationship, as viral infections are often accompanied by oxidative stress, which is a key factor in viral pathogenesis. Therefore, this study aims to analyze the potential of compounds from the white teak bark identified by Falah et al. (2008) in inhibiting SARS-CoV-2 NendoU in silico.

Materials and Methods

Materials

The materials used in this study include the 3D structure of the SARS-CoV-2 endoribonuclease (PDB ID 6WLC) downloaded from the RCSB online database (www.rcsb.org/) in *.pdb format, as well as the 3D structure of the comparison ligand tipiracil (PubChem ID 6323266) and the test ligands of the white teak bark compounds downloaded from the PubChem online database (pubchem.ncbi.nlm.nih.gov/). The test ligands include 2-(4-hydroxyphenyl)ethanol (ID 10393), 2,6-dimethoxy-p-benzoquinone (ID 68262), 3,4,5-trimethoxy-phenol (ID 69505), balanophonin (ID 23252258), and gmelinol (ID 235321). Meanwhile, the structure of (-)-p-hydroxyphenyl ethyl [5‴-O-(3,4-di-methoxycinnamoyl)-b-d-apiofuranosyl (1′→6″)]-b-d-glucopyranoside was obtained from Falah et al. (2008).

Quantitative structure-activity relationship analysis

Quantitative structure-activity relationship (QSAR) analysis was conducted to predict ligand bioactivities, especially the antioxidant and free radical scavenging activities, using Way2drug Prediction of Activity Spectra for Substances (PASS) Online web server (www.way2drug.com/passonline) (Filimonov et al., 2014).

Prediction of ligand binding sites

The potential of a protein pocket to bind a ligand was predicted using the PrankWeb (P2Rank) webserver (prankweb.cz) (Krivak & Hoksza, 2018). Protein structure in PDB format was uploaded in the entry field and set to chain A. The output is a table with information such as name, pocket score, probability score, residues in the pocket, and pocket visualization.

Protein and ligand preparation

The 3D structure of the protein was prepared using YASARA Structure (Krieger et al., 2009), which includes the removal of water molecules and unnecessary residues, addition of hydrogen atoms, removal of aliphatic hydrogen bonds, and separation of protein structure and natural ligands. The results of protein and natural ligand preparation were saved in *.pdb and *.sdf format, respectively. Meanwhile, the 3D structures of the comparison and test ligands were prepared and optimized using YASARA Structure and saved in *.sdf format (Agistia et al., 2013).

Validation of molecular docking

Validation of the docking method was performed by re-docking the natural ligand uridine-5'-monophosphate (U5P) on the protein with a grid box sized between 0.25-5.0 Å and an interval of 0.25 Å. After obtaining the docking score, the root mean square deviation (RMSD) value was determined using YASARA Structure (Siagian et al., 2022).

Visualization of molecular docking results and analysis of ligand compound characteristics

Visualization of the docking results was done in 2D with Ligplot+ (Laskowski et al., 2011) and in 3D with PyMol (Schrödinger & Delano, 2021). Meanwhile, ligand characteristics were analyzed using several online tools. Physicochemical characteristics of the ligands were predicted using the Lipinski's rule (www.scfbio-iitd.res.in/software/drugdesign/lipinski.jsp) (Lipinski, 2004). Pharmacokinetic characteristics were predicted using absorption, distribution, metabolism, excretion or ADME (www.swissadme.ch/) (Daina et al., 2017) and pkCSM tool (biosig.unimelb.edu.au/pkcsm/prediction) (Pires, et al., 2015). Prediction of the ligand toxicity was performed with AdmetSAR (lmmd.ecust.edu.cn/admetsar2/) (Cheng, et al., 2012).

Results and Discussion

Quantitative structure-activity relationship (QSAR) analysis

QSAR analysis aims to determine the relationship between the structure and biological activity of a compound (Ishikawa et al., 2012). Based on the analysis, all test ligands showed antioxidant and free radical scavenging activity with a minimum Pa value of 0.3, except gmelinol which had a Pa value of less than 0.3 in antioxidant activity (Table 1). The minimum Pa value of 0.3 indicates that the biological activity possessed by the compound is moderate (Filimonov et al., 2014; Parikesit & Nurdiansyah, 2021; Daniel et al., 2023). However, compounds with low Pa values are not necessarily certain to have low activity because not many studies have been conducted on these compounds (Ivanov et al., 2018). These results were consistent with the research done by Falah et al. (2008) which states that *Gmelina arborea* Roxb. has antioxidant activity that can inhibit cell damage, mainly through free radical scavenging properties.

Table 1. QSAR analysis of test ligands using the PASS Online server
Tabel 1. Analisis QSAR dari ligan uji menggunakan PASS Online

Canonical SMILE *Canonical SMILE*	Compound name *Nama senyawa*	Antioxidant Pa value *Nilai Pa Antioksidan*	Free radical scavenger Pa *Nilai Pa free radical scavenger*
C1=CC(=CC=C1CCO)O	2-(4-hydroxyphenyl) ethanol	0.341	0.380
COC1=CC(=O)C=C(C1=O)OC	2,6-dimethoxy-p-benzoquinone	0.439	0.499
COC1=CC(=CC(=C1OC)OC)O	3,4,5-trimethoxyphenol	0.455	0.549
COC1=C(C=C(C=C1)C2C3COC(C3(CO2)O)C4=CC(=C(C=C4)OC)OC)OC	Gmelinol	0.295	0.456
COC1=CC(=CC2=C1OC(C2CO)C3=CC(=C(C=C3)O)OC)C=CC=O	Balanophonin	0.604	0.635
COc4ccc(/C=C/C(=O)OCC3(O)COC(OCC2OC(OCCc1ccc(O)cc1)C(O)C(O)C2O)C3O)cc4OC	(-)-p-hydroxyphenyl ethyl [5‴- O-(3,4-dimethoxy cinnamoyl)-b-d-apiofuranosyl (1‴→ 6″)]- b-d-glucopyranoside	0.593	0.932

Description: Pa is the probability of belonging to the class of "actives"
Deskripsi: Pa merupakan probabilitas senyawa termasuk dalam kelompok senyawa aktif

Table 2. Prediction of ligand binding pockets with PrankWeb
Tabel 2. Prediksi kantong pengikatan ligan dengan PrankWeb

Name *Nama*	Binding pocket score *Skor kantong pengikatan*	Probability score *Skor probabilitas*	Amino acid residues *Residu asam amino*
Pocket 1	15.63	0.76	His235 Asp240 His243 Gln245 Leu246 Gly247 Gly248 His250 Lys290 Val292 Ser294 Met331 Trp333 Glu340 Thr341 Tyr343 Lys345
Pocket 2	9.05	0.53	Thr167 Thr196 Ser198 Arg199 Asn200 Leu201 Leu252 Leu266 Asp268 Met272 Asp273 Ser274 Thr275 Lys277 Tyr279 Val295 Asp297 Glu69 Lys71 Lys90
Pocket 3	6.00	0.32	Asn164 Leu43 Phe44 Glu45 Trp59 Arg62 Trp87 Tyr89 Asp92
Pocket 4	3.30	0.12	Ser162 Asn164 Gly165 Thr167 Asp273 Asn63 Val67 Glu69 Val70 Ile86 Trp87 Tyr89 Lys90
Pocket 5	3.09	0.11	Met1 Cys103 Ser104 Met105 Ser2 Leu3 Asn53 Val54 Glu57
Pocket 6	2.91	0.09	Lys159 Thr193 Tyr194 Phe195 Gln197 Arg207 Leu299 Asp302 Glu305
Pocket 7	1.98	0.04	Met210 Arg225 Tyr226 Lys227 Asp301 Val304 Glu305 Lys308
Pocket 8	1.20	0.01	Leu201 Gln202 Phe204 Pro206 Leu215 Ala256 Lys260

Description: residues labeled in yellow are the active site of the protein
Deskripsi: residu berlabel kuning merupakan sisi aktif protein

Ligand binding site prediction

Before molecular docking, prediction was done with PrankWeb (P2Rank) to determine the protein pocket position used during docking. PrankWeb (P2Rank) is a machine learning-based tool to predict ligand binding sites (Krivak & Hoksza, 2018). Predictions show that the 6WLC chain A has eight binding pockets (Figure 1a). The best pocket was determined based on pocket score, probability score, and amino acid residues found in the pocket. Pocket 1 has the highest pocket and probability scores with 12 of its 17 residues an active site of the protein (Table 2). According to Kim et al., 2021, the active site of the protein consists of catalytic and substrate binding sites. The catalytic site is composed of three residues: His250, Ser294, and Tyr343, while the substrate binding site consists of His235, Gln245, Gly248, Lys290, Val292, Cys293, Trp333, Glu340, Thr341, Pro344, Lys345, and Leu346. The similarity of the residues making up pocket 1 and the active site of the protein suggests they are in the same position (Figure 1). In addition, there is a natural ligand uridine-5'-monophosphate (U5P) docked in the pocket (Figure 1b). Therefore, molecular docking was done in pocket 1.

Structure preparation and grid box validation

Protein structure preparation was done by removing water molecules and unnecessary residues around the molecule. This aimed to reduce the potential of interference during the docking process with the ligand (Susanti et al., 2019). Ligand structures were prepared using the energy minimization method to stabilize the bond arrangement (Hanif et al., 2020) and optimize the molecular docking process.

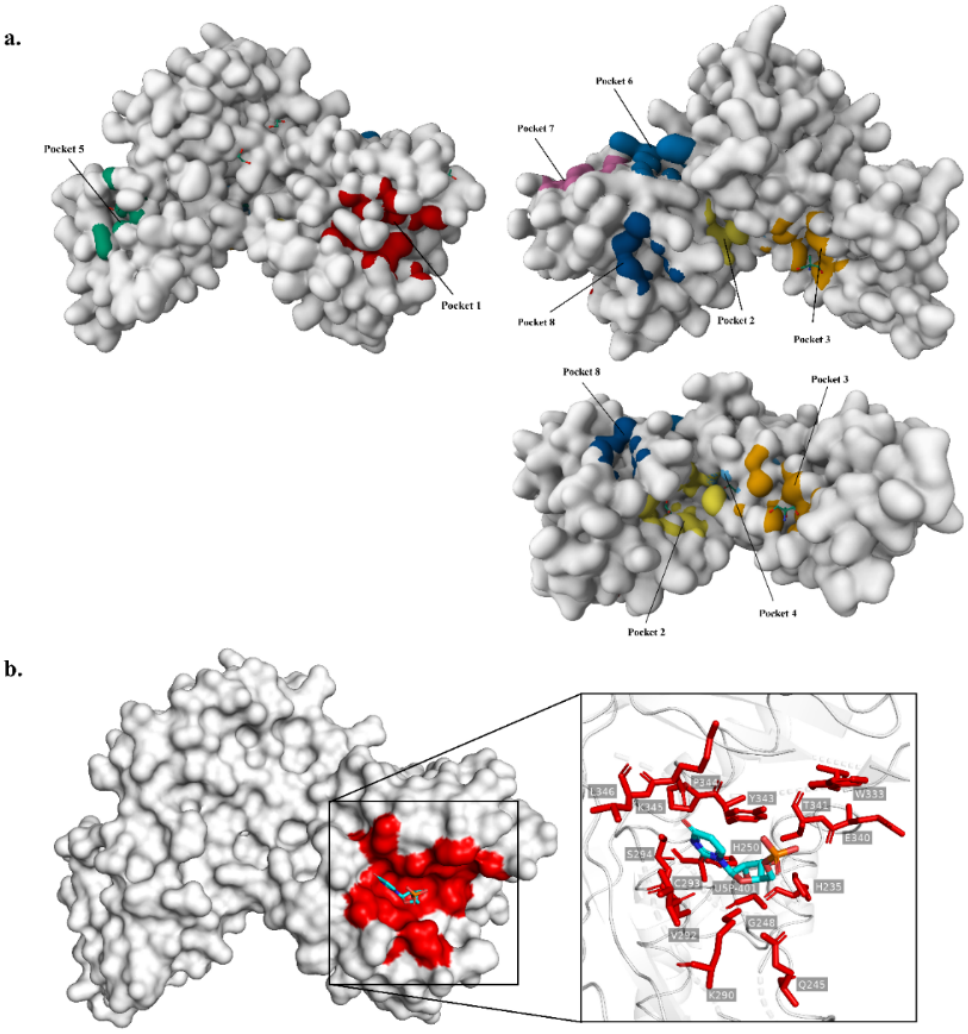

Figure 1. 3D visualization of (a) all pockets predicted by PrankWeb, (b) the active site (red) of 6WLC chain A with PyMol

Gambar 1. Visualisasi 3D (a) semua kantong pengikatan hasil prediksi PrankWeb, (b) sisi aktif (merah) 6WLC chain A dengan PyMol

After preparation, grid box validation was done with RMSD value as the parameter. RMSD value illustrates the level of deviation of the experimental ligand docking results from the crystallographic ligand on the protein binding site. The higher the RMSD value, the greater the deviation of the docked ligand position from the crystallography results (Susanti et al., 2019). Based on the analysis results, the lowest RMSD was obtained with a 2.5Å grid box size of 0.0034Å. The RMSD value was considered as valid and can be used for molecular docking of the test and comparison ligands because it is less than 3Å (Susanti et al., 2019). In addition, based on the visualization results, the pose of the validated U5P ligand overlaps with the U5P ligand in the crystallographed protein (Figure 2).

Molecular docking

Molecular docking analysis is a method of designing drug molecules using computer-aided drug discovery (CADD) techniques that aim to determine the binding pose of ligands to protein binding sites and their physicochemical interactions (Ahmed et al., 2019). The docking was carried out against the natural ligand U5P, the comparison ligand tipiracil, and the test ligands identified in the white teak bark (Falah et al., 2008). Tipiracil is a uracil-derived compound used in colorectal cancer treatment, together with trifluridine, and has been recognized by the Food and Drug Administration (FDA) (Kish & Uppal, 2016). Meanwhile, because Nsp15 (NendoU) is a uridine-specific protein, tipiracil can be used as the comparison ligand (Kim et al., 2021).

The Gibbs binding free energy (ΔG) and dissociation constant (Kd) were used as parameters to analyze the molecular docking results. The binding ΔG value describes the stability of protein-ligand complex formation (Du et al., 2016). Meanwhile, the dissociation constant is the point where all hydrogen bonds in the protein-ligand interaction are irreversibly broken (Rocheleau et al., 2016). According to Noviardi & Fachrurrazie (2015), the dissociation constant and ΔG value are directly related, so the more negative the ΔG, the smaller the Kd and the stronger and more stable the ligand-protein complex is. The docking results showed that balanophonin had the most negative ΔG and the smallest Kd compared to the other ligands (Table 3). Therefore, balanophonin is the best ligand because it inhibits the NendoU protein more potently than the natural ligand and its comparison ligands.

Figure 2. Re-docking result of natural ligand U5P in a grid box sized 2.5Å
Gambar 2. Hasil penambatan ulang ligan alami U5P pada grid box ukuran 2,5 Å

Table 3. The result of molecular docking
Tabel 3. Hasil penambatan molekuler

Compound codification *Kode senyawa*	Compund name *Nama senyawa*	Gibbs free energy of binding (kcal mol^{-1}) *Energi bebas Gibbs ikatan (kcal mol^{-1})*	Dissociation constant (μM) *Konstanta disosiasi (μM)*
L01	U5P (natural ligand)	-5.94	44.55
L02	Tipiracil (comparison ligand)	-5.90	47.66
L03	2-(4-hydroxyphenyl) ethanol	-4.72	349.24
L04	2,6- dimethoxy-p-benzoquinone	-4.73	343.97
L05	3,4,5-trimethoxyphenol	-4.49	513.16
L06	Gmelinol	-6.96	7.98
L07	Balanophonin	-7.13	5.96
L08	(-)-p-hydroxyphenyl ethyl [5‴- O-(3,4-dimethoxy cinnamoyl)-b-d-apiofuranosyl (1‴→ 6″)]- b-d-glucopyranoside	-6.06	36.32

Table 4. Protein-ligand interaction of molecular docking results
Tabel 4. Interaksi protein-ligan hasil penambatan molekul

Compound codification *Kode senyawa*	Hydrogen bond (Å) *Ikatan hidrogen (Å)*	Number of hydrogen bonds *Jumlah ikatan hidrogen*	Hydrophobic bond *Ikatan hidrofobik*	Number of hydrophobic bonds *Jumlah ikatan hidrofobik*
L01	Gly248 (4.48, 4.81) His250 (3.32, 3.84) Asn278 (4.89) Lys290 (2.96) Val292 (5.00) Ser294 (2.80, 2.94) Trp333 (3.95) Pro344 (3.75) Leu346 (3.33)	12	Gln245, Cys293, Thr341, Tyr343, Lys345	5
L02	His235 (3.33) Asp240 (4.37, 4.80) Gln245 (3.25, 4.95) His250 (3.36, 4.84) Ser294 (3.18) Thr341 (4.93)	9	Gly248, Lys290, Val292, Cys293, Tyr343, Pro344, Lys345	7
L03	His235 (3.04) Asp240 (4.37, 4.80) His250 (3.06)	4	Gly247, Gly248, Lys290, Val292, Cys293, Ser294, Thr341, Tyr343	8
L04	His250 (4.07) Ser294 (2.95)	2	Asn278, Lys290, Val292, Cys293, Tyr343, Pro344, Lys345, Leu346	8
L05	His235 (2.82) Asp240 (4.37, 4.80) Gly248 (3.29) His250 (3.02) Thr341 (3.26)	6	Gly247, Lys290, Val292, Ser294, Trp333, Tyr343	6
L06	Gly248 (3.34) His250 (4.98)	2	His235, Gln245, Leu246, Gly247, Lys290, Val292, Cys293, Ser294, Trp333, Glu340 Thr341, Tyr343, Pro344, Lys345, Leu346	15
L07	His235 (3.20) Asp240 (4.37, 4.80) Gln245 (4.53) Ser294 (2.83) Pro344 (4.69) Leu346 (3.28)	7	Leu246, Gly248, His250, Lys290, Cys291, Val292, Cys293, Thr341, Tyr343, Lys345	10
L08	His250 (4.05) Cys291 (3.73) Val292 (2.81, 3.11) Ser294 (2.99) Trp333 (3.76, 4.18) Tyr343 (3.03, 3.34)	9	His235, Gln245, Gly248, Lys290, Cys293, Met331, Thr341, Pro344, Lys345, Leu346,	10

Description: yellow-colored residues are substrate binding sites and blue colored residues are catalytic sites
Deskripsi: residu berlabel kuning berada dalam sisi pengikatan ligan dan residu berlabel biru berada dalam sisi katalitik protein

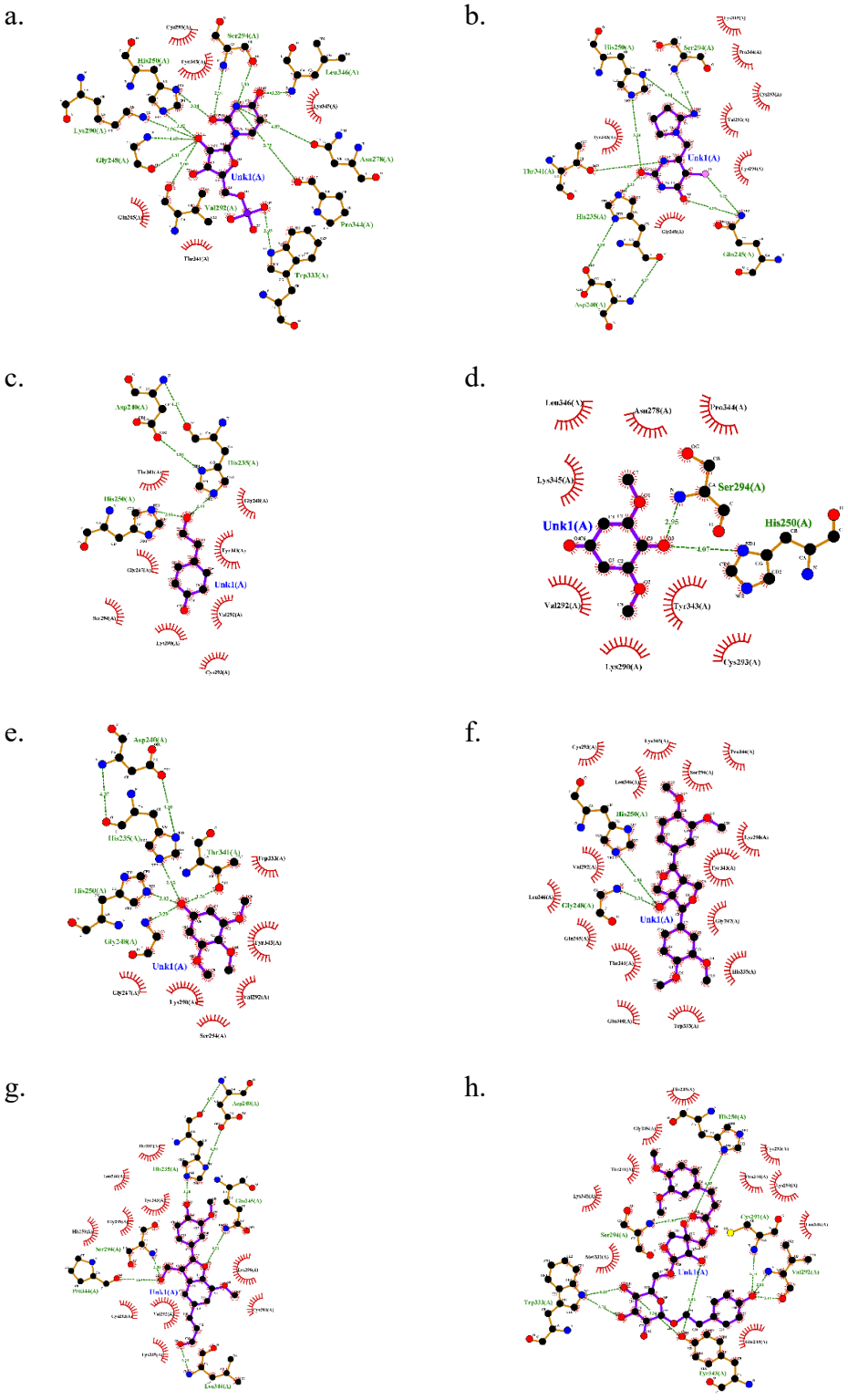

Figure 3. 2D visualization of molecular docking of (a) natural ligand uridine-5'-monophosphate; (b) comparison ligand tipiracil; (c) 2-(4-hydroxyphenyl)ethanol; (d) 2,6- dimethoxy-p-benzoquinone; (e) 3,4,5-trimethoxyphenol; (f) gmelinol; (g) balanophonin; and (h) (-)-p-hydroxyphenylethyl[5‴- O-(3,4-dimethoxycinnamoyl)-b-d-apiofuranosyl (1′→6″)]- b-d-glucopyranoside

Gambar 3. Visualisasi 2D hasil penambatan molekuler (a) ligan alami uridine-5'-monophosphate; (b) ligan pembanding tipiracil; (c) 2-(4-hydroxyphenyl)ethanol; (d) 2,6- dimethoxy-p-benzoquinone; (e) 3, 4,5-trimethoxyphenol; (f) gmelinol; (g) balanophonin; dan (h) (-)-p-hydroxyphenylethyl[5‴- O-(3,4-dimethoxycinnamoyl)-b-d-apiofuranosyl (1′→6″)]- b-d-glucopyranoside

In addition to the ΔG and Kd, the docking results can be analyzed by 2D visualization (Figure 3). Based on the analysis, the number of hydrogen and hydrophobic bonds formed was highly variable (Table 4). The difference in the number of hydrophobic interactions is because there are fewer amino acids with nonpolar side chains in the protein than polar side chains. Meanwhile, the difference in the number of hydrogen bonds is likely due to variations in the number of hydrogen bond donors and acceptors in each compound (Chen et al., 2016).

The most hydrogen bonds resulted from interactions with the natural and test ligand (L08) (-)-p-hydroxyphenyl ethyl [5‴-O-(3,4-dimethoxy-cinnamoyl)-b-d-apiofuranosyl (1‴→6″)]-b-d-glu-copyranoside (Table 3). This is because the protein used is a uridine-specific protein so the natural ligands have the most bonds with its active site (Kim et al., 2021), while the L08 ligand binds to many residues due to its large size. The large number of hydrogen bonds causes the ΔG to be more negative, thus strengthening the bond between the ligand and the protein (Tallei et al., 2020; Alimah et al., 2022). However, the most negative ΔG value is the test ligand balanophonin (L07). This may occur because the ΔG is also affected by the bond distance formed. According to Prasetiawati et al. (2021), a hydrogen bond is strong if the length is less than 2.8Å. Balanophonin and (-)-p-hydroxyphenylethyl[5‴-O-(3,4-dimethoxycinnamoyl)-b-d-apiofuranosyl (1′→ 6″)]-b-d-glucopyra-noside have hydrogen bonds with a distance of 2.8Å (Table 4). However, in balanophonin, the bond is formed on the residues that compose the protein catalytic site, making the bond more stable and resulting in more negative ΔG. Meanwhile, the most hydrophobic bonds result from interactions with gmelinol (Table 4). According to Arwansyah et al., (2014), the number of hydrophobic interactions plays a role in determining the stability of the ligand docked to the protein.

Ligand physicochemical characteristics prediction

The physicochemical characteristics of ligands can be analyzed based on Lipinksi's five rules: (1) molecular weight less than 500 Da, (2) log P value less than 5, (3) number of hydrogen bond donors less than 5, (4) number of hydrogen bond acceptors less than 10, and (5) molar refractivity ranging between 40 and 130 (Lipinski et al., 2001). Molecular weight affects the ability of compounds to passively diffuse through cell membranes because the greater the weight, the more difficult it is for molecules to pass through cell membranes. The log P value is the solubility coefficient of the compound in fat or water. The greater the logP value, the more hydrophobic the compound. The number of hydrogen bond acceptors and donors affects the amount of energy required in the absorption process (Syahputra et al., 2014). Meanwhile, the molar refractivity describes the steric properties of the compound against the protein (Marilia et al., 2021). A ligand is considered to fulfill Lipinski's rule if it does not violate more than two parameters (Petit et al., 2012). Based on the prediction results, only the ligand L08 did not pass Lipinski's rule (Table 5). Drugs that violate the Lipinski rule will cause problems in oral use and are often administered via intravenous injection (Amirian & Levy, 2020).

Ligand pharmacokinetic characteristics prediction

Absorption, distribution, metabolism, and excretion (ADME) prediction analyzes the pharmacokinetic characteristics profile of test compounds based on several parameters, including topological polar surface area (TPSA), %absorption, water solubility, GI absorption, log Kp, and bioavailability score (Nusantoro & Fadlan, 2020). TPSA estimates several ADME properties related to biological crossing barriers with acceptable values between 20 and 130Å^2 (Daina et al., 2017). Based on the analysis, only the natural ligand and L08 did

Table 5. Prediction of ligand physicochemical characteristics with Lipinski's rule
Tabel 5. Prediksi karakter fisikokimia ligan dengan aturan Lipinski

Compound codification *Kode senyawa*	Molecular weight (Da) *Berat molekul (Da)*	Log P *Log P*	Hydrogen donor *Donor hidrogen*	Hydrogen acceptor *Akseptor hidrogen*	Molar refractivity *Refraktivitas molar*
L01	324.00	-3.07	5.00	11.00	53.98
L02	242.50	-1.12	3.00	6.00	52.06
L03	138.00	0.93	2.00	2.00	38.90
L04	168.00	0.20	0.00	4.00	40.20
L05	184.00	1.42	1.00	4.00	47.77
L06	402.00	2.91	1.00	7.00	104.92
L07	356.00	3.83	2.00	6.00	95.95
L08	622.00	-0.50	6.00	14.00	150.63

Description: highlighted numbers violate Lipinski's rule
Deskripsi: nilai berlabel kuning melanggar aturan Lipinski

not meet this parameter (Table 6). Another parameter, absorption, is used to predict the amount of compound absorbed through the human small intestine. The analysis showed that all ligands had an absorption rate of more than 40% (Table 6). This indicates that all ligands are well absorbed because they have absorption values >30% (Pires et al., 2015).

Water and gastrointestinal (GI) solubility is important since the injected drug candidate must be water and gastrointestinal-soluble (Daina et al., 2017). If the compound is not sufficiently soluble in the GI, it will inhibit its absorption through the portal vein system (Lagorce et al., 2017). The analysis showed that all ligands were categorized as soluble to very soluble in water. Meanwhile, in GI solubility, the natural ligand and test ligand L08 have low solubility (Table 6). The log Kp value is a multiple linear regression that predicts the compound permeability coefficient to the skin. Compounds with low skin permeability are characterized by log Kp > -2.5 (Pires et al., 2015). Based on the results obtained, all compounds have a good level of skin permeability (Table 6). The score on the bioavailability parameter describes the ability of the test compound to reach the target site of action where at least 10% or 0.10 of the compound is present at the target (Daina et al., 2017). The analysis showed that all ligands had bioavailability scores above 0.10 (Table 6).

Prediction of ligand toxicity characteristics

Toxicity analysis was done to determine the compound potential toxic effects that can cause damage to the body after going through metabolic processes (Noviardi et al., 2020). The parameters analyzed were hERG inhibition, carcinogenicity, and acute oral toxicity. Inhibition of hERG (human Ether-a-go-go-Related Gene) causes ventricular arrhythmia in the heart (Dickson et al., 2020). Based on the analysis, only the test ligand gmelinol (L06) can cause inhibition of hERG with a probability of more than 70% (Table 7). Carcinogenicity is defined as the nature or ability of a compound to trigger neoplasia or new tissue growth (Arief et al., 2018).

Table 6. Prediction of ligand pharmacokinetic properties with ADME
Tabel 6. Prediksi karakter farmakokinetik ligan dengan ADME

Compound codification *Kode senyawa*	TPSA (Å^2) *TPSA (Å^2)*	Absorption (%) *Absorpsi (%)*	Water solubility *Kelarutan dalam air*	GI solubility *Kelarutan dalam GI*	Log Kp (cm s^{-1}) *Log Kp (cm s^{-1})*	Bioavailability score *Skor bioavailabilitas*
L01	181.12	41.00	Very Soluble	Low	-10.85	0.11
L02	92.81	67.90	Very Soluble	High	-8.26	0.55
L03	40.46	85.00	Very Soluble	High	-6.84	0.55
L04	52.60	100.00	Very Soluble	High	-7.37	0.85
L05	47.92	94.00	Soluble	High	-6.31	0.55
L06	75.61	95.00	Soluble	High	-7.42	0.55
L07	85.22	96.00	Soluble	High	-7.03	0.55
L08	203.06	41.00	Soluble	Low	-10.23	0.17

Table 7. Prediction of ligand toxicity
Tabel 7. Prediksi toksisitas ligan

Compound codification *Kode senyawa*	Parameters *Parameter*					
	hERG inhibition *Inhibisi hERG*		Carcinogenicity *Karsinogenisitas*		Acute oral toxicity *Toksisitas oral akut*	
	Category *Kategori*	Score *Skor*	Category *Kategori*	Score *Skor*	Category *Kategori*	Score *Skor*
L01	-	0.71	Non-Carcinogen	0.85	III	0.60
L02	-	0.52	Non-Carcinogen	0.86	III	0.51
L03	-	0.84	Non-Carcinogen	0.70	III	0.66
L04	-	0.75	Carcinogen	0.57	III	0.45
L05	-	0.47	Non-Carcinogen	0.63	III	0.65
L06	+	0.70	Non-Carcinogen	0.90	III	0.48
L07	-	0.42	Non-Carcinogen	0.86	III	0.57
L08	-	0.47	Non-Carcinogen	0.97	III	0.55

The analysis showed that only the test ligand 2,6-dimethoxy-p-benzoquinone (L04) was carcinogenic. Meanwhile, acute oral toxicity parameters can be determined using the LD50 value. Acute oral toxicity is exposure to a compound within 24 hours. This parameter can be categorized into 5 level groups based on the LD50 value: Ia (<5 mg/kg), Ib (5 - 50 mg/kg), II (50 - 500 mg/kg), III (500 - 2000 mg/kg) and IV (>2000 mg/kg) (Pannindriya et al., 2021). Based on the analysis results, all test compounds fall into category III, which is a safe category (Table 7).

Conclusion

Balanophonin is the best ligand because it has the most negative binding ΔG and the smallest Kd. In addition, this ligand also has good physicochemical characteristics, pharmacokinetics, and low ligand toxicity because it meets all test parameters. In conclusion, balanophonin can be developed as an effective alternative drug in inhibiting SARS-CoV-2 endoribonuclease.

References

Aditia, A. (2021). Covid-19: Epidemiologi, virologi, penularan, gejala klinis, diagnosa, tatalaksana, faktor risiko dan pencegahan. *Jurnal Penelitian Perawat Profesional*, *3*(4), 653-660. https://doi.org/10.37287/jppp.v3i4.574

Agistia, D. D., Purnomo, H., Tegar, M., & Nugroho, A. E. (2013). Interaksi senyawa aktif dari *Aegle marmelos* correa sebagai anti inflamasi dengan reseptor COX-1 dan COX-2. *Traditional Medicine Journal*, *18*(2), 80-87. https://doi.org/10.22146/tradmedj.7983

Ahmed, S., Rakib, A., Islam, M. A., Khanam, B. H., Faiz, F. B., Paul, A., Chy, M. N., Bhuiya, N. M., Uddin, M. M., Ullah, S. M., Rahman, M. A., & Emran, T. B. (2019). In vivo and in vitro pharmacological activities of *Tacca integrifolia* rhizome and investigation of possible lead compounds against breast cancer through in silico approaches. *Clinical Phytoscience*, *5*(1), 1-13. https://doi.org/10.1186/s40816-019-0127-x

Alimah, S., N., Sumaryada, T., I., Nurcholis, W., & Ambarsari, L. (2022). Molecular docking study of IPBCC.08.610 glucose oxidase mutant for increasing gluconic acid production. *JKSA, 25*(5), 169-178. https://doi.org/10.14710/jksa.25.5.169-178

Amirian, E., S. & Levy, J., K. (2020). Current knowledge about the antivirals remdesivir (GS-5734) and GS-441524 as herapeutic options for coronaviruses. *One Health, 9*, 1-7. https://doi.org/10.1016/j.onehlt.2020.100128

Arief, A., Bialangi, M. S., & Tureni, D. (2018). The level of knowledge about the dangers of smoking in students of SMP Negeri 15 Palu. *Journal of Biological Science and Education, 6*(2), 358-363. https://jurnal.fkip.untad.ac.id/index.php/ejipbiol/article/download/1060/967

Arwansyah, Ambarsari L. & Sumaryada, T.I. (2014). Simulasi docking senyawa kurkumin dan analognya sebagai inhibitor reseptor androgen pada kanker prostat. *Current Biochemistry*, *1*(11), 11-19. doi:10.29244/cb.1.1.11-19

Boopathi, S., Poma, A. B., & Kolandaivelc, P. (2020). Novel 2019 coronavirus structure, mechanism of action, antiviral drug promises and rule out against its treatment. *Journal* of *Biomolecular Structure and Dynamics*, *39*(9), 3409-3418. https://doi.org/10.1080/07391102.2020.1758788

Chen, D., Oezguen, N., Urvil, P., Ferguson, C., Dann, S. M., & Savidge, T. C. (2016). Regulation of protein-ligand binding affinity by hydrogen bond pairing. *Science Advances, 2*(3), 1-16. https://doi.org/10.1126/sciadv.1501240

Cheng, F., Li, W., Zhou, Y., Shen, J., Wu, Z., Liu, G., Lee, P. W., & Tang, Y. (2012). admetSAR: a comprehensive source and free tool for assessment of chemical ADMET properties. *Journal of Chemical Information and Modeling*, *52*(11), 3099-3105 https://doi.org/10.1021/ci300367a

Daina, A., Michielin, O., & Zoete, V. (2017). SwissADME: a free web tool to evaluate pharmacokinetics, drug-likeness and medicinal chemistry friendliness of small molecules. *Scientific Reports*, *7*(42717), 1-13. https://doi.org/10.1038/srep42717

Daniel, N., Ferdinand, F., & Aditya, P. A. (2023). In silico targeting CYP51 of *Naegleria fowleri* using bioactive compounds from Indonesian plants. *Journal of Pharmacy & Pharmacognosy Research*, *11*(5), 841-862. https://doi.org/10.56499/jppres23.1693_11.5.841

Deng, X., van Geelen, A., Buckley, A. C., O'Brien, A., Pillatzki, A., Lager, K. M., Faaberg, K. S., & Baker, S. C. (2019). Coronavirus endoribonuclease activity in porcine epidemic diarrhea virus suppresses type I and type III interferon responses. *Journal of virology*, *93*(8), e02000-18. https://doi.org/10.1128/JVI.02000-18

Dickson, C. J., Vega, C. V., & Duca, J. S. (2020). Revealing molecular determinants of hERG

blocker and activator binding. *Journal of Chemical Information and Modeling*, *60*(1), 192-203. doi.org/10.1021/acs.jcim.9b00773

Du, X., Li, Y., Xia, Y. L., Ai, S. M., Liang, J., Sang, P., Ji, X. L., & Liu, S. Q. (2016). Insights into protein-ligand interactions: Mechanisms, models, and methods. *International Journal of Molecular Sciences*, *17*(144), 1-34. https://doi.org/10.3390/ijms17020144

Falah, S., Katayama, T., & Suzuki, T. (2008). Chemical constituent from *Gmelina arborea* bark and their antioxidant activity. *Journal of Wood Science*, *54*, 483-489. https://doi.org/10.1007/s10086-008-0983-3

Fedoreyev, S., A., Krylova, N., V., Mishchenko, N., P., Vasileva, E., A., Pislyagin, E., A., Lunikhina, O., V., Lavrov, V., F., Svitich, O., A., Ebralidze, L., K., Leonova, G., N. (2018). Antiviral and antioxidant properties of echinochrome A. *Marine Drugs, 16*(12), 509-519. https://doi.org/10.3390/md16120509

Filimonov, D. A., Lagunin, A. A., Gloriozova, T. A., Rudik, A. V., Druzhilovskii, D. S., Pogodin, P. V., & Poroikov, V. V. (2014). Prediction of the biological activity spectra of organic compounds using the PASS online web resource. *Chemistry of Heterocyclic Compounds*, *50*(3), 444-457. https://doi.org/10.1007/s10593-014-1496-1

Handayani, D., Hadi, D. R., Isbaniah, F., Burhan, E., & Agustin, H. (2020). Penyakit virus corona 2019. *Jurnal Respirologi Indonesia*, *40*(2), 119-129. https://doi.org/10.36497/jri.v40i2.101

Hanif, A. U., Lukis, P. A., & Fadlan, A. (2020). Pengaruh minimisasi energi MMFF94 dengan MarvinSketch dan Open Babel PyRx pada penambatan molekular turunan oksindola tersubtitusi. *Alchemy. Journal of Chemistry, 8*(2), 33-40. https://doi.org/10.18860/al.v8i2.10481

Ishikawa, T., Hirano, H., Saito, H., Sano, K., Ikegami, Y., Yamaotsu, N., & Hirono, S. (2012). Quantitative structure-activity relationship (QSAR) analysis to predict drug-drug interactions of ABC transporter ABCG2. *Mini reviews in medicinal chemistry*, *12*(6), 505–514. https://doi.org/10.2174/138955712800493825

Ivanov, S. M., Lagunin, A. A., Rudik, A. V., Filimonov, D. A., & Poroikov, V. V. (2018). ADVERPred-web service for prediction of adverse effects of drugs. *Journal of Chemical Information and Modeling*, *58*(1), 8–11. https://doi.org/10.1021/acs.jcim.7b00568

Khan, M. T., Irfan, M., Ahsan, H., Ahmed, A., Kaushik, A. C., Khan, A. S., Chinnasamy, S., Ali, A., Wei, D. Q. (2021). Structures of SARS-CoV-2 RNA-binding proteins and theurapetic targets. *Intervirology*, *64*, 55-68. https://doi.org/10.1159/000513686

Kim, Y., Wower, J., Maltseva, N., Chang, C., Jedrzejczak, R., Wilamowski, M., Kang, S., Nicolaescu, V., Randall, G., Michalska, K., Joachimiak. (2021). Tipiracil binds to uridine site and inhibits Nsp15 endoribonuclease NendoU from SARSCoV-2. *Communication Biology, 4*(193), 1-11. https://doi.org/10.1038/s42003-021-01735-9

Kish, T., & Uppal, P. (2016). Trifluridine/tipiracil (lonsurf) for the treatment of metastatic colorectal cancer. *Pharmacy and Therapeutics*, *41*(5), 314-325.

Krieger, E. (2017). *YASARA Science Manual.* Krumbarch (DE): Frick Digitaldruck.

Krivák, R., and Hoksza, D. (2018). P2Rank: machine learning-based tool for rapid and accurate prediction of ligand binding sites from protein structure. *Journal of Cheminformatics*, *10*(39), 1-12. https://doi.org/10.1186/s13321-018-0285-8

Lagorce, D., Douguet, D., Miteva, M. A., Villoutreix, B. O. (2017). Computational analysis of calculated physicochemical and ADMET properties of protein-protein interaction inhibitors. *Scientific Reports, 7*(46277), 1-15. https://doi.org/10.1038/srep46277

Laskowski, R., A., Swindells, M., B. (2011). LigPlot+: multiple ligand-protein interaction diagrams for drug discovery. *Journal of Chemical Information and Modeling*, *51*(10), 2778-2786. https://doi.org/10.1021/ci200227u

Lipinski, C., A. (2004). Lead- and drug-like compounds: the rule-of-five revolution. *Drug Discovery Today: Technologies, 1*(4), 337-341. https://doi.org/10.1016/j.ddtec.2004.11.007

Lipinski, C., A., Lombardo, F., Dominy, B., W., Feeney, P., J. (2001). Experimental and computational approaches to estimate solubility and permeability in drug discovery and development settings. *Advanced Drug Delivery Reviews*, *46*(1), 3-26. https://doi.org/10.1016/s0169-409x(00)00129-0

Mandilara, G., Koutsi, M. A., Agelopoulos, M., Sourvinos, G., Beloukas, A., Rampias, T. (2021). The role of coronavirus RNA-processing enzymes in innate immune evasion. *Life. 11*(571), 1-17. https://doi.org/10.3390/life11060571

Marilia, V., Rusdi, B., & Fakih, T. M. (2021). Uji aktivitas senyawa apigenin dan turunannya terhadap reseptor beta-1 adrenergik sebagai antihipertensi secara *in silico. Farmasi, 7*(2), 406-415. dx.doi.org/10.29313/.v0i0.29329

Noviardi, H. & Fachrurrazie. (2015). Potensi senyawa bullatalisin sebagai inhibitor protein leukotriene A4 hidrolase pada kanker kolon secara *in silico. Fitofarmaka, 5*(2), 65-73. https://doi.org/10.33751/jf.v5i2.410

Noviardi, H., Masaenah, E., & Ramadhan, R. (2020). Penapisan molekular kandidat obat sintetik tuberkulosis terhadap protein tirosin kinase *Mycobacterium tuberculosis*. *Jurnal Farmamedika*, *5*(2), 60-69. https://doi.org/10.47219/ath.v5i2.104

Nusantoro, Y. R. & Fadlan, A. (2020). Analisis sifat mirip obat, prediksi ADMET, dan penambatan molecular isatinili-2-amniobezoil-hidrazon dan kompleks logam transisi Co(II), Ni(II), Cu(II), Zn(II) terhadap BCL2-XL. *Akta Kimindo, 5*(2), 114-126. http://dx.doi.org/10.12962/j25493736.v5i2.788

Pannindriya, P., Safithri, M., & Tarman, K. (2021). Analisis *in silico* senyawa aktif *Spirulina platensis* sebagai inhibitor tyrosinase. *JPHPI, 24*(1), 70-77. https://doi.org/10.17844/jphpi.v24i1.33122

Parikesit, A. A. & Nurdiansyah, R. (2021). Natural products repurposing of the H5N1-based lead compounds for the most fit inhibitors against 3C-like protease of SARS-CoV-2. *Journal of Pharmacy and Pharmacognosy Research*, *9*(5), 730-745. https://doi.org/10.56499/jppres21.1080_9.5.730

Petit, J., Meurice, N., Kaiser, C., & Maggiora, G. (2012). Softening the rule of five-where to draw the line?. *Bioorganic and Medicinal Chemistry*, *20*, 5343-5351. https://doi.org/10.1016/j.bmc.2011.11.064

Pires, D., E., V., Blundell, T., L., & Ascher, D., B. (2015). pkCSM: predicting small-molecule pharmacokinetic properties using graph-based signatures. *Journal of Medicinal Chemistry*, *58*(9), 4066-4072. https://doi.org/10.1021/acs.jmedchem.5b00104

Prasetiawati, R., Suherman, M., Permana, B., & Rahmawati. (2021). Molecular docking study of anthocyanidin compounds against Epidermal Growth Factor Receptor (EGFR) as anti-lung cancer. *IJPST*, *8*(1), 8-20. https://doi.org/10.24198/ijpst.v8i1.29872

Rocheleau, A. D., Cao, T. M., Takitani, T., & King, M. R. (2016). Comparison of human and mouse e-selectin binding to siayl-lewis. *BMC Structural Biology, 16*(10), 1-10. https://doi.org/10.1186/ s12900-016-0060-x

Schrödinger, L. L. C. & DeLano, W. (2021). *PyMOL*. http://www.pymol.org/pymol.

Septiana, E. (2020). Prospek senyawa bahan alam sebagai antivirus dalam menghambat SARS-CoV-2. *BioTrends*, *11*(1), 30-38.

Siagian, I., J., Purnomo, H., & Ediati, S. (2022). Study in silico compounds in sea cucumbers as immunomodulators. *JPS*, *5*(1), 33-41. https://doi.org/10.36490/journal-jps.com.v5i1.99

Susanti, N. M. P., Laksmiani, N. P. L., Noviyanti, N. K. M., Arianti, K. M., & Duantara, I. K. (2019). *Molecular docking* terpinen-4-ol sebagai antiinflamasi pada aterosklerosis secara *in silico. Jurnal Kimia*, *13*(2), 221-228. https://doi.org/10.24843/JCHEM.2019.v13.i02.p16

Syahputra, G., Ambarsari, L., & Sumaryada, T. (2014). Simulasi *docking* kurkumin enol, bisdemetoksikurkumin dan analognya sebagai inhibitor enzim 12-lipoksigenase. *Jurnal Biofisika*, *10*(1), 55 – 67.

Tallei, T., E., Tumilaar, S., G., Niode, N., J., Fatimawali, Kepel, B., J., Idroes, R., Effendi, Y., Sakib, S., A., & Emran, T., B. (2020). Potential of plant bioactive compounds as SARS-CoV-2 main protease (Mpro) and spike (S) glycoprotein inhibitors: a molecular docking study. *Scientifica,* (6307457), 1-18. https://doi.org/10.1155/2020/6307457